Vicarious radiometric calibration and validation of CBERS02B CCD data

GONG Hui[1,2], TIAN Guo-liang[1], YU Tao[1], GU Xing-fa[1], GAO Hai-liang[1], LI Xiao-ying[1]

1. *State Key Laboratory of Remote Sensing, Institute of Remote Sensing Applications, Chinese Academy of Science, Beijing* 100101, *China*;
2. *School of Civil Engineering, Beijing Jiaotong University, Beijing* 100044, *China*

Abstract: A comprehensive calibration and validation experiment of CBERS02B CCD was performed by the Center for National Spaceborne Demonstration at the Gongger site on October 12, 2007 in order to support the quantitative application program of CBERS02B data and improve the quantitative application level of CBERS02B data. The reflectance-based method was used to obtain CCD calibration coefficients for the quantitative application program of CBERS02B CCD data. The validation of the calibration coefficients was carried out at Dunhuang test site to verify reliability of the coefficients. It was shown that the vicarious calibration results were in good agreement with the measurement values. It was concluded that the calibration coefficients was highly reliable.

Key words: radiometric calibration and validation, CBERS02B CCD, calibration coefficient, reflectance-based method

CLC number: TP701 **Document code:** A

Citation format: Gong H, Tian G L, Yu T, Gu X F, Gao H L and Li X Y. 2010. Vicarious radiometric calibration and validation of CBERS02B CCD data. *Journal of Remote Sensing*, **14**(1): 001—012

1 INTRODUCTION

CBERS02B, the third transmission-type earth resource satellite jointly financed and developed by China and Brazil, was successfully launched on 19 September 2007. It added a brand-new 2.36m optical High-Resolution Panchromatic Camera (HRC) apart from reserving a 258m Wide Field Imager (WFI) and a 20m Medium Resolution CCD Camera (CCD) the same as CBERS02, which achieved complementation and combination of high and middle resolution data besides expanding application of the resource satellite. For the sake of realizing the continuity, stability and reliability of CBERS data, and improving quantitative application of CBERS02B data as well, especially monitoring of territorial resources and ecological environments, radiometric calibration, as a basic premise and key factor to quantitative remote sensing, proved to be a crucial job after launch of CBERS02B. Calibration and validation of the CBERS02B satellite data would be the precondition for their quantitative application.

Since there is not onboard calibrator for CCD, vicarious calibration is an effective method for improving accuracy and reliability of CCD data in addition to realize quantitative remote sensing of CCD data. Slater *et al.* (1987) proposed vicarious calibration methods which relied on a selected flat and uniform target at the time of sensor overpass. These methods have been proved to be highly accurate and the most in common use at present, which have been successfully used for calibrating Landsat-4,5/TM, SPOT/HRV, NOAA/AVHRR, Nimbus-7/CZCS and GOES-7/VISSR with the error of about 3%—5% (Gu, 2000). Some researchers in our country performed vicarious calibration for CBERS-02/CCD at Dunhuang test site (Li, 2006; Fu, 2005; Guo *et al.*, 2006) obtaining effective and reliable calibration coefficients with the error of 5.79% (Fu, 2005). Some scholars also proposed cross calibration (Teillet *et al.*, 2001a), in which a well-calibrated sensor regarded as a reference sensor was employed to calibrate an uncalibrated sensor. For example, CBERS-01, 02 CCD were cross-calibrated by other well-calibrated sensor such as ETM, MODIS and TM (Li *et al.*, 2005; Tang *et al.*, 2005; Yang *et al.*, 2004). But the accuracy of the method depended on some factors, such as the accuracy of well calibrated sensors, these two sensor's view to the same target at the same time and accurate match of these two sensors's spectral response and view geometry.

Based on the demand of the quantitative application program of CBERS02B data, a comprehensive calibration and validation experiment of CBERS02B CCD was performed by the Center for National Spaceborne Demonstration at the Gongger site on October 12, 2007. Reflectance-based calibra-

Received: 2009-01-06; **Accepted**: 2009-05-20

Foundation: "863"program supported by the National High Technology Research and Development Program of China No.8-060011.

First author biography: GONG Hui (1971—), female, doctoral student. She gets M.S. in Changchun University of Science and Technology in 1999. Her research interests include radiometric calibration and quantitative remote sensing. Currently, 5 representative papers haven been published. E-mail: gonghuiyue@sohu.com

tion method was used for calibration of CBERS02B CCD at the Gongger site and the result was validated by using Dunhuang test site.

Parameter setting of CBERS02B CCD is shown in Table 1.

Table 1 Main parameters of CBERS02B CCD

Band	Wavelength /μm	Spacial resolution /m	Swath /km	Sideways pointing capability /(°)	Revisit period /d	IFOV /(°)
1	0.45—0.52					
2	0.52—0.59					
3	0.63—0.69	20	113	±32	26	8.32
4	0.77—0.89					
5	0.51—0.73					

2 METHOD AND EXPERIMENT

2.1 Reflectance-based calibration method (Biggar, 1990)

Reflectance-based calibration method was based on the ground measurements of surface reflectance over the natural target, solar extinction measurements in addition to sounding and meteorologic observations made at the time of the CBERS02B overpass on the site. After processing of these data and match of spectral response between CCD and surface instrument, some results were achieved. The results were input to radioactive transfer code (Vermote *et al.*, 1997), to estimate the top-of-atmosphere (TOA) radiance or TOA reflectance for CCD band. Calibration coefficient of CCD band was estimated by comparing the TOA radiance or TOA reflectance with average digital count of the CCD image.

The equivalent spectral radiance L_i for CCD band i was defined as (Li, 2006)

$$L_i = \int_{\lambda_1}^{\lambda_2} R(\lambda) \times L_i(\lambda) \mathrm{d}\lambda / \int_{\lambda_1}^{\lambda_2} R(\lambda) \mathrm{d}\lambda \quad (1)$$

where $R(\lambda)$ was the spectral response of the CCD band at wavelength λ, $L_i(\lambda)$ was TOA radiance of the CCD band at wavelength λ.

The calibration coefficient of CCD was be derived by the relation between the TOA radiance L_i and the average digital count for pixels corresponding to the ground by the following expression:

$$L_i = (\mathrm{DC}_i - \mathrm{DC}_{0i}) / a_i \quad (2)$$

where a_i was gain, DC_{0i} was offset, DC_i was digital count of CCD band i.

The TOA radiance L_i could be expressed as the TOA reflectance as (Vermote *et al.*, 1997):

$$\rho_i^*(\theta_s, \theta_v, \varphi_s, \varphi_v) = (\pi L_i(\theta_s, \theta_v, \varphi_s, \varphi_v)(r/r_0)^2) / E_{0i}\mu_s \quad (3)$$

where θ_s, θ_v, φ_s, φ_v was respectively the solar and view zenith and azimuth angles, L_i was TOA radiance of CCD band i, E_{0i} was the extra-atmospheric solar spectral irradiance at the mean distance of the earth and sun, and (r/r_0), the earth-sun factor, was the ratio of the real earth-sun distance to mean distance, $\mu_s = \cos\theta_i$.

For a uniform lambertian ground of surface reflectance ρ_i, the TOA reflectance ρ_i^* was given as (Vermote *et al.*, 1997)

$$\rho_i^*(\theta_s, \theta_v, \varphi_s, \varphi_v) = [\rho_{Ai}(\theta_s, \theta_v, \varphi_s, \varphi_v) + (\tau_i(\mu_s)\rho_i\tau_i(\mu_v))/(1 - \rho_i s_i)]T_{gi} \quad (4)$$

where ρ_{Ai} was the upward scattering reflectance of the atmosphere for CCD band i, τ_i was the global atmospheric transmittance, ρ_i was the surface reflectance, s_i was the spherical albedo of the atmosphere, and T_{gi} was the transmittance of absorptive gas.

Under the condition of nadir sun irradiance and at the mean distance of the earth and sun, TOA reflectance calibration formulation could be expressed as:

$$\rho_i^{**}(\theta_s, \theta_v, \varphi_s, \varphi_v) = (\mathrm{DC}_i - \mathrm{DC}_{0i}) / c_i \quad (5)$$

where c_i was gain and DC_{0i} was offset of digital count for CCD band i.

The flow chart of the reflectance-based calibration method was shown in Fig. 1.

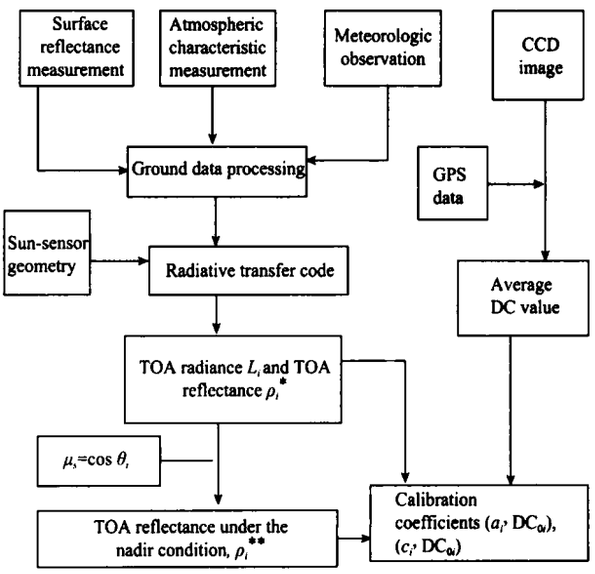

Fig. 1 Flow chart of the reflectance-based calibration method

2.2 Experiment

2.2.1 *The test site*

The Gongger test site, a part of the Huailai test site network, is located at north of Dalinoer Lake in Keshiketeng Banner of Inner Mongolia (Fig. 2) with an elevation of 1.27km. It belongs to middle-latitude drought continental monsoon climate. Average annual precipitation here is only 294.9 mm while evaporation is as high as 2000mm. Total sunshine in these places are as long as 3066.4h and average cloud cover is 3.875. These facts mean it is sunny and dry in most time of each year (Gao *et al.*, 2007). The site has a quite wide area and a flat surface which is about 4km wide and 5km long. The composition of surface is

sandy loam soil covered with low vegetation which has been withered and yellow during the experiment time. It could be seen from reflectance results which were derived from 50 surface samples in the 2km×2km area in May 2007 and 1800 surface samples in the 400m×400m area in October 2007, that average relative error of reflectance in visible and near-infrared bands for the site was 3.5%—3.7%. These facts show that surface condition and atmospheric characteristic of the site are fit for calibration during spring and autumn. According to the condition of the site and characteristic of CBERS02B, a section of 400m×400m area of the site was chosen for the calibration of CBERS02B CCD.

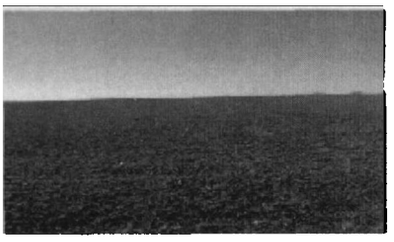

Fig. 2 The Gongger test site

2.2.2 Surface spectra measurements

Surface spectra measurements were performed at the site at the time of CBERS02B overpass on Oct 12, 2007. It took two hours to collect spectra data for the whole site. The Analytical Spectral Devices (ASD) Spectrometer was used to obtain the surface spectra. The spectrometer covered the entire solar reflected wavelength range from 350nm to 2500nm with approximately 3 nm (VNIR) and 10 nm (SWIR) spectral resolution (David, 2002). In order to obtain surface spectral data as more as possible, the spectrometer was arranged to automatically collect the spectral data at 2s intervals along the longitude and latitude directions, during which the panel spectra was measured every 6min. At the same time, GPS was used to position and track the instrument for accurate surface position. About 3600 spectra data were collected for the site.

2.2.3 Atmospheric characteristic measurements

Atmospheric measurements were made at the place 2 km away from the test site at the measurement time to obtain atmospheric total optical depth, aerosol optical depth, content of ozone and total column water vapor. Atmospheric aerosol optical depth was retrieved from the measurement by an automatic sun tracking photometer CE318, whose arm was to collect spectral solar direct irradiance data from 7am to 5pm. CE318's band setting was shown in Table 2 (Yuan *et al.*, 2006). Total column water vapor was obtained with sounding view outline. The content of ozone came from NASA TOMS data (Richard, 2007).

Table 2 CE318's band setting

Band	1	2	3	4	5	6	7	8
Center wavelength /nm	1020	1640	870	670	440	500	936	340
Band width /nm	10	60	10	10	10	10	10	2

3 DATA PROCESSING AND RESULT ANALYSIS

3.1 Surface spectral data processing and analysis

In order to diminish the influence of solar irradiance to the measured value and of automatic measurement mode to the error of spectral data, 3600 spectra data were divided into groups at 1min interval. Mean surface spectrum was obtained by averaging all of surface spectral data in a group during one minute. In the meantime, the panel spectral data were interpolated at the interval of one minute corresponding to the time of mean surface spectra. Afterwards, BRF of panel was interpolated according to solar zenith angle at the measurement time. Then absolute surface reflectance could be obtained by the expression (Zhang *et al.*, 2001)

$$\rho(\lambda)=\frac{v(\lambda)}{v_s(\lambda)}\rho_s(\lambda) \tag{6}$$

where $\rho_s(\lambda)$ was spectral reflectance of the panel, $v_s(\lambda)$ and $v(\lambda)$ were respectively raw digital counts of panel and target on the same view condition.

A representative spectral reflectance for the site at the time of overpass on Oct 12, 2007 was obtained after averaging spectral reflectances of all ground samples. It was shown in Fig. 3 in wavelength range from 400nm to 1100nm. It was noted from Fig. 3 that the surface reflectance held slow and steady increase in CCD visible and near-infrared bands. On the one hand, it presented the characteristic of soil which accounted for little effect of vegetation on surface reflectance. On the other hand, it denoted that surface reflectance kept good spectral homogeneity. 3.7% relative error also indicated that the surface was spatial homogeneous. In other words, the site was fit for radiometric calibration.

The reflectance spectra obtained above was changed into the equivalent spectral reflectance for CCD band by using the equation (Li, 2006):

$$\rho_i=\frac{\int_{\lambda_1}^{\lambda_2}\rho(\lambda)R_i(\lambda)\mathrm{d}\lambda}{\int_{\lambda_1}^{\lambda_2}R_i(\lambda)\mathrm{d}\lambda} \tag{7}$$

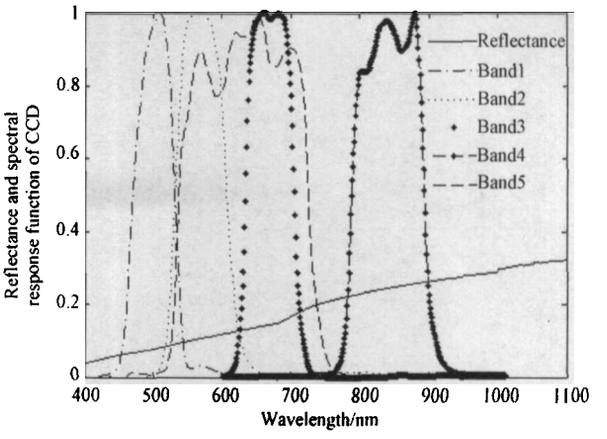

Fig. 3 Surface reflectance results of the test site and spectral response function of CCD

where $\rho(\lambda)$ was the average spectral reflectance at λ, $R_i(\lambda)$ was the relative spectral response for CCD band i. the equivalent spectral reflectance of CCD 4 bands was 0.54% and average relative error was 3.8%.

3.2 CE318 data processing and result analysis

According to spectral solar direct irradiance and diffuse irradiance measured with CE318, atmospheric aerosol optical depth for CE318 channel was determined using a Langley method. The result was shown in Fig. 4(a). It can be seen from the figure that the aerosol content changed little from 9 am to 1 pm which indicated that atmospheric condition was fairly stable. After assuming that the aerosol followed Junge distribution, atmospheric aerosol optical depth at channel 440nm and channel 870nm was used to retrieve Ångström turbidity coefficient, β, and wavelength exponent, α, as shown in Fig. 4(b). Then aerosol optical depth at 550nm wavelength could be estimated from the Ångström parameters. Parameter α explained the change of aerosol particle's composition during the view time. The large value of the parameter accounted for high content of small particles and vice versa. Parameter β noted the concentration of aerosol. The smaller the value of β was, the cleaner the atmosphere was and the sunnier it was. It can be indicated from Fig. 4 (b) that the sky was clear and temporally stable all the day. Aerosol was mainly macroparticle and had low concentration. Alteration of β corresponded with the change of aerosol optical depth. The above-mentioned facts showed that there was little change for aerosol optical depth and aerosol affected slightly to atmospheric radiative transfer.

3.3 Calibration coefficients calculation and analysis

Calibration coefficient was obtained by relating TOA radiance or TOA reflectance with digital count. Based on the preceding results, some parameters could be gained. They included the surface reflectance, sun-target-sensor geometries and the atmospheric parameters including aerosol optical depth for band 550nm, total column water vapor and the content of ozone. Then TOA reflectance (ρ_{TOA} as shown in Table 4) or TOA radiance (L_{TOA} as shown in Table 4) could be obtained by inputting these parameters into a radioactive transfer code, 6S. Geometry and atmospheric characteristic parameters were shown in Table 3.

Table 3 Geometry and atmospheric characteristic parameters at the time of CCD overpass on Oct 12, 2007

View time	Solar zenith angle /(°)	Solar azimuth agle /(°)	Spectrol optical depth (550nm)	Total column water vapor /(g/cm^2)	Ozone content /(D.U.)
10:16—12:16	51.17	166.16	0.094	0.634	291

On the other hand, after geometric rectification with GPS data, the area in the CCD image corresponding to the measured ground was defined and average digital count for the area was obtained by averaging digital count values of all pixels in the area. Relative error of about 2% for digital count value illustrated that the ground was very homogeneous. Since the offset DC_{0i} had been cancelled from CCD image in the course of relative radiometric correction, that is to say, digital count of the image was just the value (DC_i–DC_{0i}) existing in Eq.(2) and Eq.(5). Furthermore, TOA radiance or TOA reflectance for CBERS02B CCD were gained after dividing the value (DC_i–DC_{0i}) by calibration coefficient. Then according to comparison of average digital count with TOA radiance or TOA reflectance simulated from 6S, calibration coefficient for CCD band could be achieved by using Eq.(2) and Eq.(5), as shown in Table 4 together with prelaunch coefficient.

By comparing calibration coefficient of vicarious calibration with that of prelaunch, it could be seen that vicarious calibration results, especially band 1 and band 2, existed large difference with those of prelaunch, for which the largest relative error value was about 31% except for band 3. It was inferred that all bands of CBERS02B CCD underwent some change to different degrees. The responses of band 1 and band 2 varied too much with the difference more than 20% due to the change of environment while the response of band 3 was relative stable with the neglectable difference of 1.93% after launch.

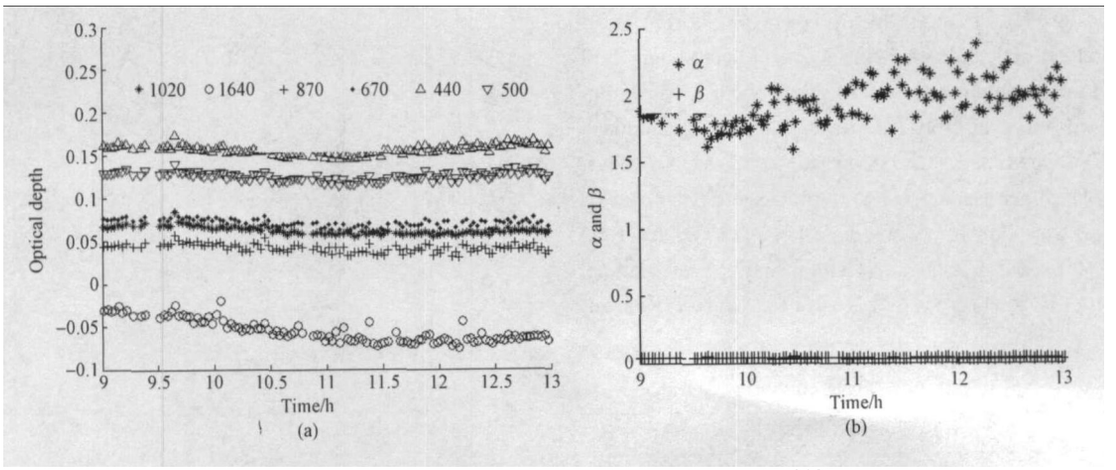

Fig. 4 Optical properties of atmospheric aerosol on Oct 12, 2007
(a) Aerosol optical depth changed with time; (b) Parameters

Table 4 Results of both preflight calibration and the vicarious calibration on Oct 12, 2007

Band	B_1	B_2	B_3	B_4	B_5
DC value ot the site	52.26	43.78	68.25	78.72	48.88
ρ_{TOA}	0.125	0.125	0.148	0.232	0.140
c_i	419.08	350.82	462.4	339.6	350.13
L_{TOA}/(W·m^{-2}·sr^{-1}·μm^{-1})	47.96	45.25	44.91	48.3	45.67
a_i/(DN/W·m^{-2}·sr^{-1}·μm^{-1})	1.09	0.968	1.52	1.63	1.07
Prelaunch calibration coefficients	1.43	1.396	1.491	1.809	1.02
Relative error/%	−23.80	−30.68	1.93	−9.90	4.92

3.4 Error analysis

For the reflectance-based method, there are many error sources, such as the measurement of ground surface, the assumption of a lambertian characteristic for the ground, the measurement of atmospheric parameters, the assumption and the calculation of radiometric transfer code. The root sum of squares is generally used to define the total error generated from various error sources (Biggar *et al.*, 1994). It could be confirmed after simulation for main error sources that the error from measurement of surface reflectance shared the biggest source for total error and transferred error equivalently. After analyzing and simulating the above error sources, the uncertainty of the calibration campaign for CBERS02B CCD was less than 6% as shown in Table 5.

Table 5 Reflectance-based calibration uncertainty for CCD

	Overall error/%
Surface reflectance	3.8
Non-lambertain ground characteristic	1.5
Optical depth measurement	1.5
Aerosol type	2.0
Complex refractive index of aerosols	1.5
Absorptive gas	1.4
Inherent accuracy of model	2.0
Correction of scattered light	1.5
Uncertainty of the solar zenith angle	0.2
Total error (root sum of squares)	5.7

3.5 Validation

To verify the reliability of the calibration coefficients simulated above, independent data obtained at the Dunhuang test site on Oct 21, 2007 were used. TOA radiance estimated from the in-situ measurements at the Dunhuang test site was regarded as standard value just shown as L_i^* from 6S in Table 6. CCD image-based TOA radiance achieved independently using the vicarious calibration coefficient above was compared with the standard value to verify the reliability of the calibration coefficient. The result was shown in Table 6. It was noted from Table 6 that TOA radiance calculated from vicarious calibration coefficient was in quite good agreement with the standard value, which indicated that vicarious calibration coefficient was highly reliable. It was a favorable precondition for the later quantitative application research of CBERS02B CCD. On the other hand, the preflight results existed large disagreement with the standard value after comparison, especially band 1 and band 2. It confirmed further that there indeed were changes in the response of band 1 and band 2 after launch. The conclusion agreed very well to the result at the Gongger test site. It indicated that it was absolutely indispensable to monitor the change of the response of the sensor with vicarious calibration method.

4 CONCLUSION

According to the above work, some conclusions could be achieved as following.

(1) Based on the real-time measurement at the Gongger site, radiometric calibration for CBERS02B CCD was successfully

Table 6 Comparison of TOA radiances between simulated from calibration coefficients and obtained from ground measured data

Band	B_1	B_2	B_3	B_4	B_5
DC value of Dunhuang test site	81.61	66.99	99.6	82.62	71.87
TOA radiance from vicarious calibration/(W·m^{-2}·sr^{-1}·μm^{-1})	74.89	69.22	65.54	50.69	67.16
TOA radiance from prelaunch calibration/(W·m^{-2}·sr^{-1}·μm^{-1})	57.07	47.98	66.80	45.67	70.46
TOA radiance from 6S/(W·m^{-2}·sr^{-1}·μm^{-1})	76.09	73.63	65.66	47.00	67.10
Absolute error between TOA radiance from vicarious calibration and from 6S/(W·m^{-2}·sr^{-1}·μm^{-1})	−1.20	−4.40	−0.12	3.69	0.06
Relative error/%	−1.58	−5.98	−0.18	7.84	0.09

performed using reflectance-based calibration methods and calibration coefficients for CCD bands were obtained as well. These achievements laid the foundation for quantitative application research of CBERS02B CCD data and were useful to improve the application of CCD data as well.

(2) It was concluded from surface reflectance data from multi-year and multi-spot: Gongger test site was fairly flat and homogeneous and its average error was 3.5%—3.7%. It was fit for calibration for CBERS02B during spring and autumn. Near distance and convenient communication to Beijing provided new calibration test site for sensor with high resolution.

(3) According to contrast and analysis for results from both vicarious calibration and the prelaunch, it was confirmed that the response of CCD changed at some extent after launch, especially band 1 and band 2. As a result, it was quite essential to update calibration coefficient timely and periodically in order to monitor the change of CBERS02B CCD better.

(4) As for validation result estimated from the real-time measurement at the Dunhuang site, TOA radiance from vicarious calibration of CCD was consistent with the standard value. The result indicated that vicarious calibration coefficient was very good and reliable with high application value.

Acknowledgements: The authors wish to acknowledge David and Qin Yi from Marine and Atmospheric Research of Commonwealth Scientific and Industrial Research Organisation and Li Li, Zang Wenqian and Sun Wei from the Center for National Space-borne Demonstration for their works in the campaign. We are also grateful to the China Center for Resource Satellite Data and Applications for the access to the CCD data and to Fu Qiaoyan and Qi Xueyong for the field data support of Dunhuang test site.

REFERENCES

Biggar S F, Slater P N and Gellman D I. 1994.Uncertainties in-flight calibration of sensors with reference to measured ground sites in the 0.4 to 1.1μm range. *Remote Sensing of Environment*, **48**: 245—252

Biggar S F. 1990. Cross Methods for Satellite Sensor Absolute Radiometric Calibration. America: the University of Arizona

David C H. Analytical spectral devices.2002. Inc. HandHeld Spectroradiometer User's Guide

Fu Q Y. 2005. In-flight absolute calibration research of resource satellite: based on the Dunhuang test site experiment for CBERS-02 in 2004. Beijing: Normal University

Gao H L, Zhang Y X, Gu X F, Yu T, Gong H and Zhu L. 2007. Surface characterization analysis of Inner Mongolia Plateau area (China) as potential satellite calibration Sites using MODIS(Terra and Aqua) instrument. IGRASS07, 1420—1423

Gu M L. 2000. In-flight absolute radiometric calibration of satellite remote sensor. *Spacecraft Recovery & Remote Sensing*, **21**(1): 16—21

Guo J N, Min X J, Fu Q Y, Li X C, Pan Z Q, Feng C, Guo Y, Huang S C, Li Q M and Tang W P. 2006. The in-flight absolute calibrations for CBERS-02 CCD and SPOT-4 HRVIR1 sensors at Dunhuang test site and the comparison based on their coefficients. *Journal of Remote Sensing*, **10**(5): 624—629

Li X Y, Gu X F, Min X J, Yu T, Fu Q Y, Zhang Y and Li X W. 2005. Radiometric cross-calibration of the CBERS-02 CCD camera with the TERRA MODIS. *Science in China Ser. E*, **48**(supp): 44—60

Li X Y. 2006. In Flight Radiometric Calibration and Pixel Based Calibration for CCD Camera and WFI Imager on CBERS-02 Beijing: Chinese Academy of Sciences

Richard D M. What is the total column ozone amount you're your house? http://toms.gsfc.nasa.gov/teacher/ozone_overhead_v8.html. (2007-11-12)

Slater P N, Biggar S F, Holm R G, Jackson R D, Mao Y, Moran M S, Palmer J M and Yuan B. 1987. Reflectance- and radiance-based methods for the cross absolute calibration of multispectral sensors. *Remote Sensing of Environment*, **22**(1): 11—37

Tang J W, Gu X F, Niu S L, Ma C F and Min X J. 2005. Water target based cross-calibration of CBERS-02 CCD camera with MODIS data. *Science in China Ser. E*, **48**(supp): 61—71

Teillet P M, Fedosejevs G, Gauthier R P, O'Neill N T, Thome K J, Biggar S F, Ripley H and Meygret A. 2001a. A generalized approach to the vicarious calibration of multiple Earth observation sensors using hyperspectral data. *Remote Sensing of Environment*, **77**: 304—327

Vermote E, Tanré D, Deuzé J L, Herman M and Morcrette J J. 1997. Second Simulation of the Satellite Signal in the Solar Spectrum(6S). 6S User Guide Version 2

Yang Z D, Gu S Y, Qiu Hong, Huang Q and Fan T X. 2004. CBERS-1's CCD image quality evaluating and cross calibration study. *Journal of Remote Sensing*, **8**(2): 113—120

Yuan H J, Gu X F, Chen L F Yu T, Liu Q and Li X W. 2006. Retrieval and analysis of aerosol optical thickness over Qianyanzhou Region. *Journal of Remote Sensing*, **10**(5): 762—769

Zhang J P, Yi W N, Wang X H, Qiao Y L and Zheng X B. 2001. Measurement and analysis of reflectance in central area of Dunhuang radiometric calibration site. Compilation of Papers about Scientific Research Achievement for China Radiometric Calibration Sites. Beijing: Geological Publishing Press

CBERS02B 卫星 CCD 相机在轨辐射定标与真实性检验

巩　慧[1,2], 田国良[1], 余　涛[1], 顾行发[1], 高海亮[1], 李小英[1]

1.中国科学院 遥感应用研究所 遥感国家重点实验室, 北京 100101;
2.北京交通大学 土建学院, 北京 100044

摘　要: 利用贡格尔实验场对 CBERS02B 卫星进行场地反射率基法辐射定标, 获得 CCD 相机可见近红外波段的绝对辐射定标系数, 利用敦煌实验场对定标系数进行了真实性检验。结果表明: 此次定标结果和测量值非常吻合, 定标系数可信度高。

关键词: 辐射定标与真实性检验, CBERS02B 卫星 CCD 相机, 定标系数, 反射率基法

中图分类号: TP701　　**文献标识码:** A

引用格式: 巩慧, 田国良, 余涛, 顾行发, 高海亮, 李小英. 2010. CBERS02B卫星CCD相机在轨辐射定标与真实性检验. 遥感学报, 14(1): 001—012

Gong H, Tian G L, Yu T, Gu X F, Gao H L and Li X Y. 2010. Vicarious radiometric calibration and validation of CBERS02B CCD data. *Journal of Remote Sensing*, 14(1): 001—012

1　引　言

中巴地球资源卫星 02B 星(简称 CBERS02B 卫星)于 2007-09-19 成功发射, 这是中国、巴西两国政府共同投资、联合研制的第 3 颗传输型地球资源卫星。星上有效载荷除保留中巴地球资源卫星 02 星上 20m 分辨率的 CCD 相机和 258m 分辨率的 WFI 相机外, 新增分辨率为 2.36m 的高分辨率(HR)相机, 实现了中、高分辨率数据的互补与结合, 拓展了资源卫星的应用领域。为了实现数据的连续性、稳定性、可靠性, 提高 CBERS02B 卫星数据的遥感定量化应用水平, 尤其是资源、生态环境的遥感监测, 卫星传感器的辐射定标作为遥感定量化的前提和关键环节, 成为 CBERS02B 卫星发射后的一项重要工作。

由于 CBERS02B 卫星没有星上定标系统, 在轨辐射定标成为提高该卫星数据的准确度和可靠性、实现卫星数据遥感定量化的有效手段。以美国亚利桑那大学光学科学中心 Slater 教授为代表的科学家提出利用地表大面积均匀稳定的地物目标进行传感器的在轨场地辐射定标方法(Slater, 1987)是定标精度较高的方法, 也是目前国际上最常用的绝对辐射定标方法(顾名澧, 2000)。这种方法已成功地对 Landsat-4、5 卫星的 TM、SPOT 卫星的 HRV、NOAA-9、10、11 卫星的 AVHRR、Nimbus-7 卫星的 CZCS 以及 GOES-7 卫星的 VISSR 进行了辐射定标, 在可见光和近红外波段的定标精度可达 3%—5%左右(顾名澧, 2000)。中国的一些研究人员曾通过此方法在敦煌实验场对 CBERS-02 卫星上的 CCD 相机进行辐射定标(李小英, 2006; 傅俏燕, 2005; 郭建宁等, 2006), 获得了有效可靠的定标系数以及 5.79%的定标精度(傅俏燕, 2005)。一些学者也采用交叉定标(Teillet 等, 2001a), 以 ETM、MODIS、TM 的传感器为标准, 对 CBERS-01、02 卫星的 CCD 相机进行定标研究(李小英等, 2005; 唐军武等, 2005; 杨忠东等, 2004), 但交叉定标的精度依赖于标准传感器的精度、2 个传感器对同一目标的同时观测以及相互之间的光谱及观测几何的精确匹配。

国家航天局航天论证中心基于 CBERS02B 卫星

收稿日期: 2009-01-06; **修订日期:** 2009-05-20

基金项目: 国家 863 无场地定标关键技术项目(编号: 8-060011)。

第一作者简介: 巩慧(1971—), 女, 博士生, 1999 年毕业于长春科技大学遥感技术应用专业, 获硕士学位, 现从事定量遥感、遥感传感器辐射定标的理论和应用研究, 已发表论文 5 篇。E-mail: gonghuiyue@sohu.com。

数据的定量化应用示范研究项目的需求，于2007年10月在北京怀来综合实验场网的内蒙古贡格尔实验场开展 CBERS02B 卫星场地定标与真实性检验工作。针对 CBERS02B 卫星 CCD 相机，采用场地反射率基辐射定标法进行辐射定标，利用敦煌实验场进行定标系数的真实性检验。

CBERS02B 卫星 CCD 相机的参数设置见表 1。

表 1 CBERS02B 卫星 CCD 相机的主要技术参数

谱段	波长范围 /μm	空间分辨率 /m	幅宽 /km	侧摆能力 /(°)	重访时间 /d	视场角 /(°)
1	0.45—0.52					
2	0.52—0.59					
3	0.63—0.69	20	113	±32	26	8.32
4	0.77—0.89					
5	0.51—0.73					

2 方法和实验

2.1 反射率基辐射定标方法(Biggar, 1990)

反射率基法是当CBERS02B卫星飞越实验场上空时，在地面进行地表反射比、场地周围大气消光和探空气象的同步观测以及场区各采样点定位信息的获取。然后对这些观测数据进行处理、星-地光谱响应匹配，获得辐射定标计算所需的中间参数。将这些中间参数输入 6S 辐射传输模型(Vermote 等, 1997)，计算得到 CCD 相机各通道入瞳处的 TOA 辐亮度和 TOA 反射率，同时在 CCD 相机图像上提取观测区的平均计数值，将 TOA 辐亮度和 TOA 反射率分别与图像的平均计数值比较得到相应的 CCD 相机各通道定标系数。

对于 CCD 相机通道 i 测量的等效 TOA 辐亮度 L_i 为(李小英, 2006):

$$L_i = \int_{\lambda_1}^{\lambda_2} R(\lambda)\times L_i(\lambda)\mathrm{d}\lambda / \int_{\lambda_1}^{\lambda_2} R(\lambda)\mathrm{d}\lambda \quad (1)$$

式中，$R(\lambda)$为 CCD 相机归一化的光谱响应函数，$L_i(\lambda)$为通道 i 波长 λ 处的 TOA 辐亮度。

对于 CCD 相机，其等效 TOA 辐亮度 L_i 与 CCD 相机探测到的计数值 DC_i 的关系为:

$$L_i = (DC_i - DC_{0i})/a_i \quad (2)$$

式中，a_i 为增益，DC_{0i} 为计数值的偏移量。

CCD 相机入瞳处各通道的 TOA 辐亮度用 TOA 反射率ρ_i^*可表示为(Vermote 等, 1997):

$$\rho_i^*(\theta_s,\theta_v,\varphi_s,\varphi_v) = (\pi L_i(\theta_s,\theta_v,\varphi_s,\varphi_v)(r/r_0)^2)/E_{0i}\mu_s \quad (3)$$

式中，θ_i, θ_v, φ_i, φ_v 分别为太阳、卫星的天顶角和方位角，L_i 为 TOA 辐亮度，E_{0i} 为大气外界太阳辐照度，(r_0/r)为平均与实际日-地距离之比，μ_s ($\mu_s = \cos\theta_i$)为太阳天顶角的余弦。

对于朗伯特性较好的地面目标，TOA 反射率ρ_i^*可表示为(Vermote 等, 1997):

$$\rho_i^*(\theta_s,\theta_v,\varphi_s,\varphi_v) = [\rho_{Ai}(\theta_s,\theta_v,\varphi_s,\varphi_v) + (\tau_i(\mu_s)\rho_i\tau_i(\mu_v))/(1-\rho_i s_i)]T_{gi} \quad (4)$$

式中，ρ_{Ai} 为大气本身产生的向上的散射反射率，τ_i 是大气自身透过率，ρ_i 为地表反射率，s_i 为大气球反照率，T_{gi} 为吸收气体透过率。

在太阳垂直入射、平均日-地距离条件下，TOA 反射率ρ_i^{**}与 CCD 相机图像计数值关系为:

$$\rho_i^{**}(\theta_s,\theta_v,\varphi_s,\varphi_v) = (DC_i - DC_{0i})/c_i \quad (5)$$

式中 c_i 为增益，DC_{0i} 为计数值的偏移量。

反射率基法定标流程如图 1。

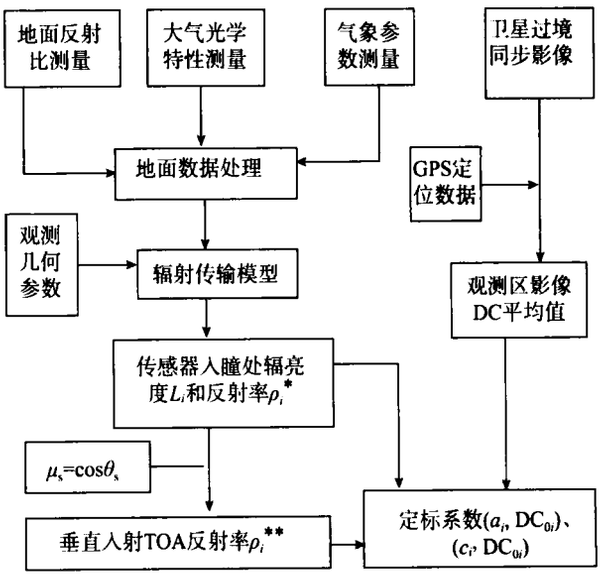

图 1 反射率基法定标流程图

2.2 实 验

2.2.1 场区介绍

贡格尔实验场属于北京怀来实验场网的一部分，位于内蒙古克什克腾旗达里诺尔湖北侧(图 2)，平均海拔 1266m，属中温带大陆性季风气候，年平均降水量只有 294.9mm，年蒸发量可达 2000mm，年日照数长达 3066.4h，天空总云量平均为 3.875，大气洁净干燥(高海亮等, 2007)。场区面积广阔，地势平坦，东西宽约 4km，南北长约 5km，地表层为黄色沙壤土，覆有低矮草类，此时已枯黄。根据 2007 年 5 月在实验区 2km×2km 的观测区域共 50 个地面点进行

的同步观测处理结果和 2007 年 10 月在实验区 400m×400m 的观测区域共 1800 个地面点的同步观测处理结果可知，场区反射比在可见光和近红外波段的平均相对差异为 3.5%—3.7%。说明贡格尔实验场的气候、大气及地表条件适合在春秋季节进行在轨场地辐射定标。根据场区的情况以及 CBERS02B 星的特点，选择 400m×400m 的观测区域作为 CBERS02B 卫星 CCD 相机辐射定标同步实验区。

图 2　贡格尔实验场

2.2.2　地面光谱测量

CBERS02B 卫星于 2007-10-12 11:16 过贡格尔草原实验场上空，当天在贡格尔实验场进行了地面光谱准同步测量，观测时间为卫星过顶前后 1h。地表光谱的测量采用 FR ASD 野外光谱仪，FR ASD 野外光谱仪光谱范围为 350—2500nm，光谱分辨率为 VNIR: 3nm; SWIR: 10nm(David, 2002)。为了尽可能多地获取地面数据，仪器采取自动测量模式，时间间隔为 2s，沿经纬度方向采集地表光谱数据，大约每隔 6min 进行白板测量，同时利用 GPS 进行定位跟踪，获取精确的地表定位数据。整个同步测区共获取 3600 组光谱数据。

2.2.3　大气光学特性测量

同步观测当天在距离场地 2km 处进行大气消光和探空观测，以获得场区上空大气总消光光学厚度和气溶胶消光光学厚度、臭氧、水汽含量等大气光学参数。气溶胶光学厚度的测量利用自动跟踪太阳光度计 CE318，测量时间从 7:00—17:00。CE318 光度计的波段配置见表 2(袁海军等, 2006)。水汽含量的测量利用探空观测，除常规 2 次探空观测外，在卫星过境时刻增加 1 次无线电探空观测。臭氧含量来自 NASA TOMS 数据(Richard, 2007)。

表 2　CE318 波段配置

波段配置	1	2	3	4	5	6	7	8
中心波长/nm	1020	1640	870	670	440	500	936	340
波段宽度/nm	10	60	10	10	10	10	10	2

3　数据结果处理与分析

3.1　地表光谱数据处理与分析

为减少太阳辐照度变化对测值的影响以及自动测量模式对测量数据造成的误差，对野外获取的 3600 组光谱数据进行处理时，以 1min 为间隔，将每 1min 内的地表光谱测值进行平均得到地表光谱平均值，同时将参考板的测量数据按照 1min 进行插值处理，将地表光谱平均值时间插值后的参考板值的时间一一对应，再对参考板 BRF 按测量时刻太阳天顶角进行插值计算，根据式(6)获得地表绝对反射比 $\rho(\lambda)$ (章俊平等, 2001):

$$\rho(\lambda)=\frac{v(\lambda)}{v_s(\lambda)}\rho_s(\lambda) \tag{6}$$

式中，$\rho_s(\lambda)$是参考板的实际光谱反射比，$v_s(\lambda)$和 $v(\lambda)$分别是相同条件下参考板和测量目标所得到的计数值。

将所有的地表绝对反射比平均得到场地平均反射比光谱曲线，如图 3(波段范围 400—1100nm)。从图 3 可以看出，场地反射比在可见光、近红外波段呈现缓慢、平稳上升的特点，表现为土壤光谱曲线，说明此时地表植被的状况没有影响地表反射比；同时位于 CCD 相机各波段的光谱响应范围内的地表反射比变化平稳缓慢，说明场地反射比在 CCD 相机各波段的光谱响应范围内具有较好的光谱均匀性。场地反射比测量的平均相对差异为 3.7%，表明场地具有较好的均匀性。以上结果表明场地适合定标。

利用公式(7)将场地绝对反射比数据与 CCD 相机各通道的光谱响应函数进行积分，即获得 CCD 相机各通道相应的地面等效反射率(李小英, 2006):

$$\rho_i=\frac{\int_{\lambda_1}^{\lambda_2}\rho(\lambda)R_i(\lambda)\mathrm{d}\lambda}{\int_{\lambda_1}^{\lambda_2}R_i(\lambda)\mathrm{d}\lambda} \tag{7}$$

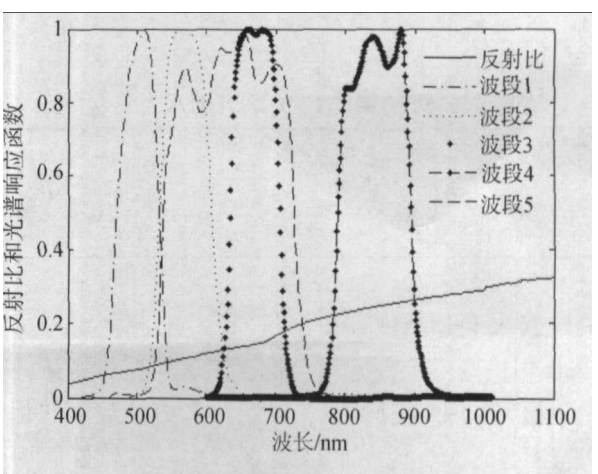

图 3　地表反射比和 CCD 光谱响应函数

式中，ρ_i为CCD相机波段i的等效地表反射率；$R_i(\lambda)$为CCD相机波段i的光谱响应函数。4个波段的等效反射率的平均误差0.54%，平均相对差异为3.8%。

3.2 CE318数据处理与分析

根据CE318上半天测量的直射太阳辐射和天空辐射数据，采用Langley方法反演得到CE318各通道的大气气溶胶光学厚度如图4(a)。可以看出，自9:00—13:00期间气溶胶含量变化很小，表明大气状况稳定。假定气溶胶谱为龙格(Junge)分布，利用440nm和870nm 2个通道的气溶胶光学厚度计算得到波长指数α和浑浊系数β(图4(b))，由此导出550nm波长处的气溶胶光学厚度。波长指数α反映了观测期间大气中气溶胶粒子组成的变化，α大，表明小粒子含量较多；α小，表明大粒子含量较多。β则反映了气溶胶浓度的大小，β越小表明能见度越好，大气越清洁，天气也越晴朗。图4(b)显示出观测当天实验场区大气晴好稳定，大粒子气溶胶为主，浓度很低，大气清洁、能见度很好，气溶胶对辐射传输的影响小，β曲线的变化趋势与气溶胶光学厚度的变化趋势非常吻合，均表现出气溶胶变化极小的特点。

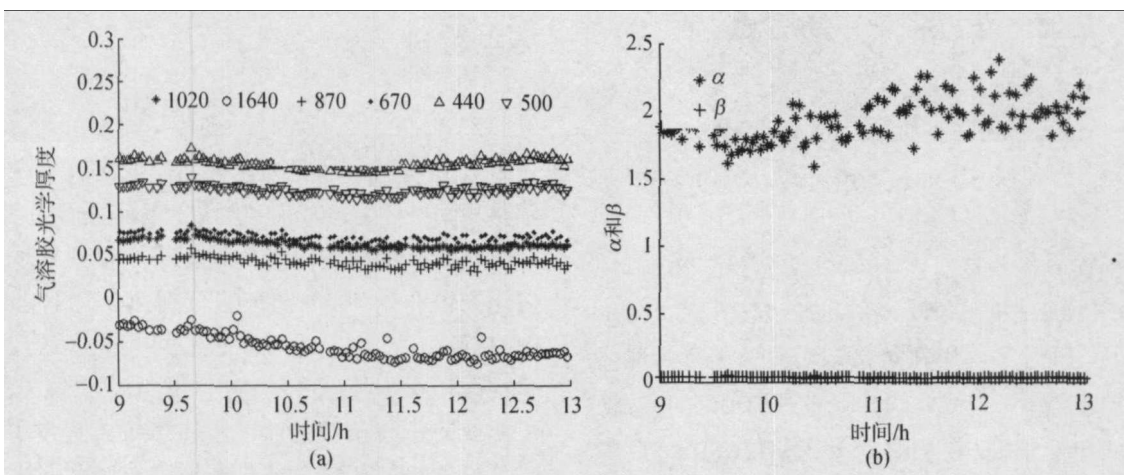

图4 2007-10-12大气气溶胶光学特征

(a) 各通道气溶胶光学厚度随时间变化；(b) 波长指数(α)和浑浊系数(β)

3.3 定标系数计算与分析

定标系数是通过将测区的TOA辐亮度和TOA反射率分别与图像的平均计数值比较得到的，在上述工作的基础上，首先将得到的CCD相机通道的地面等效反射率、大气气溶胶光学厚度、水汽含量、臭氧含量以及太阳和卫星几何观测条件等参数输入到6S辐射传输模型，获得CCD相机各通道的TOA反射率(ρ_{TOA})和TOA辐亮度(L_{TOA})。卫星几何参数和大气光学特性参数如表3。

表3 2007-10-12 CCD的几何和大气参数

同步观测时间	太阳天顶角/(°)	太阳方位角/(°)	气溶胶光学厚度(550nm)	水汽含量/(g/cm^2)	臭氧含量/(D.U.)
10:16—12:16	51.17	166.16	0.094	0.634	291

其次利用GPS数据进行星-地测区配准，在CCD相机图像上圈定出与地面测区对应的区域并提取该区域的平均计数值，得到测区内计数值的相对差异约为2%，说明测区地表的均匀性较好。由于CCD相机在进行相对辐射校正时已去除发射前测出的通道计数值偏移量DC_{0i}，即图像的计数值已为式(2)和式(5)中的(DC_i-DC_{0i})部分，且CBERS02B卫星CCD相机的TOA辐亮度和TOA反射率是利用(DC_i-DC_{0i})除以相应的定标系数来得到，因此根据图像平均计数值和6S计算得到的TOA辐亮度和TOA反射率，利用式(2)、式(5)得到CCD相机各通道辐亮度和反射率的定标系数。获得各通道定标系数和发射前的定标系数对比结果见表4。

对比辐亮度的场地定标系数和发射前定标系数可以看出，除CCD相机波段3的场地定标系数和发射前定标系数变化不大外，其他波段，尤其是波段

表4 发射前定标结果和场地定标结果(2007-10-12)

波段	B_1	B_2	B_3	B_4	B_5
场地DN值	52.26	43.78	68.25	78.72	48.88
$\rho_{TOA\_场地}$	0.125	0.125	0.148	0.232	0.14
c_i	419.1	350.8	462.4	339.6	350.1
$L_{TOA\_场地}$ /(W·m^{-2}·sr^{-1}·μm^{-1})	47.96	45.25	44.91	48.3	45.67
a_i/(DN/ W·m^{-2}·sr^{-1}·μm^{-1})	1.09	0.97	1.52	1.63	1.07
发射前定标系数	1.43	1.396	1.491	1.809	1.02
相对差异/%	−23.80	−30.68	1.93	−9.90	4.92

1、波段 2 的场地定标系数和发射前定标系数相差很大，最大相对差异达到近 31%，表明 CBERS02B 卫星 CCD 相机各个波段有不同程度的变化，除波段 3 在卫星发射前后性能稳定外，由于卫星发射前后运行环境的变化，波段 1 和波段 2 的性能变化较明显。

3.4　误差分析

在反射率基辐射定标方法中，误差有多种来源，如地面反射比测量、地面朗伯特性假设、大气参数及探空测量误差、模型的假设和辐射传输模型计算产生的误差等。通常用平方和的根表示对参与定标误差源的不确定度的估算(Biggar 等, 1994)。经过对参与定标的主要误差源进行模拟计算，认为地表反射比测量误差在总误差源中贡献最大，并且它的误差贡献基本上是等量传递的。通过对上述误差源分析和模拟计算，本次 CBERS02B 星 CCD 相机的场地反射率基法外辐射定标的不确定度小于 6%，具体误差分析见表 5。

表 5　CCD 相机场地反射率基法外辐射定标误差分析

	总误差贡献/%
地面反射比	3.8
非朗伯地面特性	1.5
光学厚度测量	1.5
气溶胶类型选择	2.0
气溶胶复折射指数	1.5
吸收气体	1.4
模型固有精度	2.0
野外漫射光校正	1.5
太阳天顶角误差不确定性	0.2
总误差(平方和的根)	5.7

3.5　真实性检验

为了检验本次定标系数的真实性和可靠性，以 2007-10-21 CBERS02B 卫星过敦煌实验场的地面同步测量数据计算得到的 TOA 辐亮度作为比较的基准值，利用本次得到的定标系数和 2007-10-21 敦煌实验场的 CBERS02B 卫星 CCD 图像的计数值计算出 TOA 辐亮度，将计算的 TOA 辐亮度与基准值进行比较，验证定标系数的真实性和可靠性，结果如表 6。由表 6 看出：各波段计算的 TOA 辐亮度和基准值之间的差异很小，说明本文得到的定标系数可信度高，这为 CBERS02B 卫星 CCD 相机后续的定量化应用研究提供了良好的前提。将发射前定标系数计算得到的 TOA 辐亮度与基准值比较，波段 1、波段 2 存在很大的差异，进一步证实了 CBERS02B 卫星 CCD 相机波段 1、波段 2 在卫星发射前后发生了较大变化，这与上面的定标系数结果分析一致，表明了在轨定标对监测传感器变化的必要性。

表 6　利用定标系数计算的 2007-10-21 敦煌场 TOA 辐亮度和测量值的比较

波段	B_1	B_2	B_3	B_4	B_5
CCD 图像 DN 值	81.61	66.99	99.6	82.62	71.87
场地定标系数计算的 TOA 辐亮度 /(W·m^{-2}·sr^{-1}·μm^{-1})	74.89	69.22	65.54	50.69	67.16
发射前定标系数计算的 TOA 辐亮度 /(W·m^{-2}·sr^{-1}·μm^{-1})	57.07	47.98	66.80	45.67	70.46
TOA 辐亮度基准值 /(W·m^{-2}·sr^{-1}·μm^{-1})	76.09	73.63	65.66	47.00	67.10
计算值与测量值之差 /(W·m^{-2}·sr^{-1}·μm^{-1})	−1.20	−4.40	−0.12	3.69	0.06
相对差异/%	−1.58	−5.98	−0.18	7.84	0.09

4　结　论

根据以上围绕 CBERS02B 卫星数据的定量化应用示范研究项目开展的 CBERS02B 卫星 CCD 相机的定标与真实性检验研究，可以得到以下结论：

(1) 通过本次在贡格尔实验场的场地同步观测，采用场地反射率基辐射定标法成功地对 CBERS02B 卫星的 CCD 相机各波段进行辐射定标研究，得到了 CCD 相机各波段的辐射定标系数，为 CBERS02B 卫星 CCD 相机数据的定量化应用示范研究奠定了基础，有利于提高 CCD 相机数据的应用水平；

(2) 实验场的多年多点地表反射比数据证明：贡格尔实验场地表平坦均一，反射率平均误差 3.5%—3.7%，可用于 CBERS02B 卫星在春秋季节的定标；由于贡格尔实验场距离北京较近，交通方便，为高分辨率传感器多次定标提供了新的定标场地；

(3) 通过本次场地试验辐射定标系数与发射前实验室辐射定标系数的对比分析，CCD 相机存在一定的变化，尤其是波段 1 和波段 2，为更好地监测 CBERS02B 卫星 CCD 相机的变化，及时、定期地更新辐射定标系数十分必要；

(4) 利用敦煌实验场的同步测量数据进行真实性检验的结果表明：利用 CCD 相机的场地定标系数计算的 TOA 辐亮度和基准值非常接近，表明这一定标结果比较理想，定标系数可信度高，具有较高的应用价值。

致　谢　此次野外实验的数据获取得到了澳大利亚科学与工业研究组织大气与海洋研究所 David

和秦益以及国家航天局航天论证中心李丽、孙伟、藏文前同学的协助，CCD 图像数据的获取得到资源卫星应用中心相关部门的大力支持，同时资源卫星应用中心傅俏燕、亓雪勇在数据验证方面提供了帮助和支持，在此表示衷心的感谢！

REFERENCES

Biggar S F, Slater P N and Gellman D I. 1994.Uncertainties in-flight calibration of sensors with reference to measured ground sites in the 0.4 to 1.1 μm range. *Remote Sensing of Environment*, **48**: 245—252

Biggar S F. 1990. Cross Methods for Satellite Sensor Absolute Radiometric Calibration. America: the University of Arizona

David C H. Analytical spectral devices.2002. Inc. HandHeld Spectroradiometer User's Guide

Fu Q Y. 2005. In-flight absolute calibration research of resource satellite: based on the Dunhuang test site experiment for CBERS-02 in 2004. Beijing: Normal University

Gao H L, Zhang Y X, Gu X F, Yu T, Gong H and Zhu L. 2007. Surface characterization analysis of Inner Mongolia Plateau area (China) as potential satellite calibration Sites using MODIS(Terra and Aqua) instrument. IGRASS07, 1420—1423

Gu M L. 2000. In-flight absolute radiometric calibration of satellite remote sensor. *Spacecraft Recovery & Remote Sensing*, **21**(1): 16—21

Guo J N, Min X J, Fu Q Y, Li X C, Pan Z Q, Feng C, Guo Y, Huang S C, Li Q M and Tang W P. 2006. The in-flight absolute calibrations for CBERS-02 CCD and SPOT-4 HRVIR1 sensors at Dunhuang test site and the comparison based on their coefficients. *Journal of Remote Sensing*, **10**(5): 624—629

Li X Y, Gu X F, Min X J, Yu T, Fu Q Y, Zhang Y and Li X W. 2005. Radiometric cross-calibration of the CBERS-02 CCD camera with the TERRA MODIS. *Science in China Ser. E*, **48**(supp): 44—60

Li X Y. 2006. In Flight Radiometric Calibration and Pixel Based Calibration for CCD Camera and WFI Imager on CBERS-02 Beijing: Chinese Academy of Sciences

Richard D M. What is the total column ozone amount you're your house? http://toms.gsfc.nasa.gov/teacher/ozone_overhead_v8.html. (2007-11-12)

Slater P N, Biggar S F, Holm R G, Jackson R D, Mao Y, Moran M S, Palmer J M and Yuan B. 1987. Reflectance- and radiance-based methods for the cross absolute calibration of multispectral sensors. *Remote Sensing of Environment*, **22**(1): 11—37

Tang J W, Gu X F, Niu S L, Ma C F and Min X J. 2005. Water target based cross-calibration of CBERS-02 CCD camera with MODIS data. *Science in China Ser. E*, **48**(supp): 61—71

Teillet P M, Fedosejevs G, Gauthier R P, O'Neill N T, Thome K J, Biggar S F, Ripley H and Meygret A. 2001a. A generalized approach to the vicarious calibration of multiple Earth observation sensors using hyperspectral data. *Remote Sensing of Environment*, **77**: 304—327

Vermote E, Tanré D, Deuzé J L, Herman M and Morcrette J J. 1997. Second Simulation of the Satellite Signal in the Solar Spectrum(6S). 6S User Guide Version 2

Yang Z D, Gu S Y, Qiu H, Huang Q and Fan T X. 2004. CBERS-1's CCD image quality evaluating and cross calibration study. *Journal of Remote Sensing*, **8**(2): 113—120

Yuan H J, Gu X F, Chen L F, Yu T, Liu Q and Li X W. 2006. Retrieval and analysis of aerosol optical thickness over Qianyanzhou Region. *Journal of Remote Sensing*, **10**(5): 762—769

Zhang J P, Yi W N, Wang X H, Qiao Y L and Zheng X B. 2001. Measurement and analysis of reflectance in central area of Dunhuang radiometric calibration site. Compilation of Papers about Scientific Research Achievement for China Radiometric Calibration Sites. Beijing: Geological Publishing Press

附中文参考文献

傅俏燕. 2005. 资源卫星在轨绝对辐射定标方法研究——以 2004 年 CBERS-02 星敦煌场地实验为例. 北京: 北京师范大学

顾名澧. 2000. 星载传感器在飞行时的绝对辐射定标方法. 航天返回与遥感, **21**(1): 16—21

郭建宁, 闵祥军, 傅俏燕, 李杏朝, 潘志强, 冯春, 郭毅, 黄世存, 李启明, 汤伟平. 2006. CBERS-02 CCD 和 SPOT-4 HRVIR1 两个传感器的敦煌场地在轨绝对辐射定标及对比分析. 遥感学报, **10**(5): 624—629

李小英, 顾行发, 闵祥军, 余涛, 傅俏燕, 张勇, 李小文. 2005. 利用 MODIS 对 CBERS-02 卫星 CCD 相机进行辐射交叉定标. 中国科学 E 辑, **35**(增刊): 41—58

李小英. 2006. CBERS-02 卫星 CCD 相机与 WFI 成像仪在轨辐射定标与像元级辐射定标研究. 北京: 中国科学院

唐军武, 顾行发, 牛生丽, 马超飞, 闵祥军. 2005. 基于水体目标的 CBERS-02 卫星 CCD 相机与 MODIS 的交叉辐射定标. 中国科学 E 辑, **35**(增刊): 59—69

杨忠东, 谷松岩, 邱红, 黄签, 范天锡. 2004. 中巴地球资源一号卫星 CCD 图像质量评价和交叉定标研究. 遥感学报, **8**(2): 113—120

袁海军, 顾行发, 陈良富, 余涛, 刘强, 李小文. 2006. 江西千烟洲地区气溶胶光学厚度的反演与分析. 遥感学报, **10**(5): 762—769

章俊平, 易维宁, 李先华, 乔延利, 郑小兵. 2001. 敦煌辐射校正场中心区反射率特性的测量及分析. 中国遥感卫星辐射校正场科研成果论文选编. 北京: 地质出版社